Detection and Identification of Faulty Sensors in Dynamic Processes

S. Joe Qin and Weihua Li
Dept. of Chemical Engineering, University of Texas, Austin, TX 78712

A novel method proposed detects and identifies faulty sensors in dynamic systems using a subspace identification model. A consistent estimate of this subspace model was obtained from noisy input and output measurements by using errors-in-variables subspace identification algorithms. A parity vector was generated, which was decoupled from the system state, leading to a model residual for fault detection. An exponentially weighted moving average (EWMA) filter was applied to the residual to reduce false alarms due to noise. To identify faulty sensors, a dynamic structured residual approach with maximized sensitivity is proposed which generates a set of structured residuals, each decoupled from one subset of faults but most sensitive to others. All the structured residuals are also subject to an EWMA filtering to reduce the noise effect. Confidence limits for filtered structured residuals were determined using statistical inferential techniques. Other indices like generalized likelihood ratio and cumulative variance were compared to identify different types of faulty sensors. The fault magnitude was then estimated based on the model and faulty data. Data from a simulated 4×4 process and an industrial waste-water reactor were used to test the effectiveness of this method, where four types of sensor faults, including bias, precision degradation, drift, and complete failure, were tested.

Introduction

Existing work in sensor validation can be divided into three categories: (i) gross-error detection and identification based on open-loop first principles models; (ii) closed-loop observer or Kalman filter-based sensor fault detection and isolation; and (iii) multivariate statistics based sensor validation using methods like principal component analysis (PCA) and partial least squares (PLS). Usually, three tasks are involved in sensor validation, including detection, identification, and reconstruction of the faulty sensors using available information.

Published work in gross error detection and identification is reviewed thoroughly in Crowe (1996). Mah et al. (1976), Stanley and Mah (1977, 1981), and Romagnoli and Stephanopoulos (1981) are among the early works in gross error detection and rectification in chemical processes. Crowe et al. (1983) propose a matrix projection approach to eliminate unmeasured variables present in the balance equations. Rollins and Davis (1992) propose an unbiased estimation technique (UBET) for the estimation of fault magnitudes. Dynamic gross error detection is studied by a number of researchers (Albuquerque and Biegler, 1996; Karjala and Himmelblau, 1996; Liebman et al., 1992). These methods typically formulate the detection of gross errors as a nonlinear program. Because a nonlinear model is involved, the computational cost is high and the unique identification of the gross errors is often not guaranteed.

The literature of fault detection and isolation contains a plethora of methods for sensor validation, which often treats sensor validation as a specific task of the general fault detection problem. Most methods in this category are based on dynamic state observers or Kalman filters. Deckert et al. (1997) applied redundant hardware sensors to detect and identify abnormal sensors in an F-8 airplane. Chow and Willsky (1984) used state space models to generate parity equations for fault detection and isolation. Frank and Wunnenberg (1989) used unknown input observers to deal with process and sensor fault detection and isolation. Some of the methods reviewed in Frank and Ding (1997) are relevant to sensor validation. The use of process parity equations to gen-

Correspondence concerning this article should be addressed to S. J. Qin.

erate structured residuals is described in Gertler and Singer (1990), Gertler (1991), and Gertler and Kunwer (1995). A structured residuals approach with maximized sensitivity for fault isolation at steady state was proposed by Qin and Li (1999).

The use of multivariate statistical methods for sensor validation received significant attention. Originally proposed as a process monitoring technique in Jackson (1991) and Kresta et al. (1991), the PCA and PLS methods are effective for sensor validation based on normal process data. Sensor fault identification is made possible by the use of contribution plots (Miller et al., 1993; Tong and Crowe, 1995) and a sensor validity index (SVI) via reconstruction (Dunia et al., 1996). Recent work by Gertler et al. (1999) uses a set of PCA models to enhance fault isolation. The work by Tong and Crowe (1995) is among the first to apply PCA to analysis of the model residuals. Relations between several principal component tests and other traditional tests are also given. A related data-based method is the use of auto-associative neural networks as a nonlinear PCA for sensor validation in Kramer (1991). Fantoni and Mazzola (1994) apply the work of Kramer (1991) to the sensor validation of nuclear power plants. In these methods, quasi-steady-state models are used to detect sensor gross errors.

The fact that existing methods for sensor validation received only restricted use in practice is due to one or several of the following limitations: (i) an accurate first principles model is required *a priori*; (ii) there is not enough sensitivity to uniquely identify the faulty sensors from normal ones; (iii) the methods are not robust to process disturbances and other measurement errors; and (iv) only a quasi-steady-state situation is considered. In this article, we propose a new optimal method for the detection and identification of faulty sensors in dynamic processes using a normal subspace model. This model is consistently identified using errors-in-variables (EIV) subspace model identification (SMI) algorithms (Chou and Verhaegen, 1997) from noisy input and output measurements. This method can also be applied to dynamic models built from the first principles. Given a normal process model, we generate a parity vector that is decoupled from the system state and contains a linear combination of current and previous inputs and outputs. By manipulating the parity vector, we generate a residual for fault detection. An exponentially weighted moving average (EWMA) filter is applied to the residual to reduce false alarms due to noise. To identify which sensor is faulty, a *dynamic structured residual approach with maximized sensitivity* (DSRAMS) is proposed to generate a set of residuals where one residual is most sensitive to one specified subset of faults, but insensitive to others. All the structured residuals are also subject to EWMA filtering to reduce the effect of noise. The confidence limits for these filtered structured residuals (FSRs) are determined using statistical techniques. By comparing the FSRs against their respective confidence limits, faulty sensors can be readily identified. In addition, in order to identify different types of faults, other indices such as the generalized likelihood ratio (GLR) and the cumulative variance (Vsum) are applied and compared. After the identification of the faulty sensors, the fault magnitude is then estimated based on the model and faulty data, and the faulty sensors are reconstructed. Data from a simulated process and an industrial wastewater reactor are used to test the effectiveness of the proposed scheme, where four types of sensor faults, including bias, precision degradation, drifting, and complete failure are simulated.

The design is described of a model residual for fault detection that is decoupled from the state variables. Details of the DSRAMS method for fault identification are given, including fault identification indices, the optimal estimate of the fault magnitude, and the reconstruction of faulty sensors based on the normal model and faulty data. An errors-in-variables subspace identification approach tailored for fault detection and identification is proposed. Two case studies on a simulated dynamic process and an industrial wastewater reactor process are carried out before the conclusions are given.

Fault Detection in Dynamic Systems

A state space model is used to formulate the dynamic fault detection problem. In the formulation we assume measurement noise is present in both output and input sensors. Process noise is also included in this formulation. The model can be derived using a subspace identification method that handles the errors-in-variables (EIV) situation (Chou and Verhaegen, 1997), but it can also be derived from first principles. Since in model predictive control applications a dynamic model is already available, we will also discuss the use of a dynamic transfer function model or finite impulse response (FIR) model for fault detection.

Model and fault representation

A general errors-in-variables dynamic process model can be represented by the following state space formulation (Chou and Verhaegen, 1977)

$$\begin{aligned} \boldsymbol{x}(t+1) &= \boldsymbol{A}\boldsymbol{x}(t) + \boldsymbol{B}[\boldsymbol{u}(t) - \boldsymbol{v}(t)] + \boldsymbol{p}(t) \\ \boldsymbol{y}(t) &= \boldsymbol{C}\boldsymbol{x}(t) + \boldsymbol{D}[\boldsymbol{u}(t) - \boldsymbol{v}(t)] + \boldsymbol{o}(t) \end{aligned} \tag{1}$$

where $\boldsymbol{u}(t) \in \Re^l$, $\boldsymbol{y}(t) \in \Re^m$, and $\boldsymbol{x}(t) \in \Re^n$ are input, output and state variables, respectively; $\boldsymbol{A}$, $\boldsymbol{B}$, $\boldsymbol{C}$ and $\boldsymbol{D}$ are system matrices with appropriate dimensions. $\boldsymbol{v}(t)$, $\boldsymbol{o}(t)$ and $\boldsymbol{p}(t)$ are input, output and process noises, respectively. By manipulating Eq. 1, we obtain

$$\begin{aligned} \boldsymbol{y}_s(t) = \boldsymbol{\Gamma}_s \boldsymbol{x}(t-s) + \boldsymbol{H}_s \boldsymbol{u}_s(t) - \boldsymbol{H}_s \boldsymbol{v}_s(t) \\ + \boldsymbol{G}_s \boldsymbol{p}_s(t) + \boldsymbol{o}_s(t) \end{aligned} \tag{2}$$

where the extended observability matrix $\boldsymbol{\Gamma}_s$ and other matrices are defined as

$$\boldsymbol{\Gamma}_s = \begin{bmatrix} \boldsymbol{C} \\ \boldsymbol{CA} \\ \vdots \\ \boldsymbol{CA}^s \end{bmatrix} \in \Re^{m_s \times n} \tag{3}$$

$$\boldsymbol{H}_s = \begin{bmatrix} \boldsymbol{D} & & & \\ \boldsymbol{CB} & \boldsymbol{D} & & \\ \vdots & & \ddots & \\ \boldsymbol{CA}^{s-1}\boldsymbol{B} & & & \boldsymbol{D} \end{bmatrix} \in \Re^{m_s \times l_s} \tag{4}$$

$$G_s = \begin{bmatrix} \mathbf{0} & & & \\ C & \mathbf{0} & & \\ \vdots & & \ddots & \\ CA^{s-1} & & & \mathbf{0} \end{bmatrix} \in \Re^{m_s \times n_s} \tag{5}$$

The *extended* vectors $y_s(t)$, $v_s(t)$, $o_s(t)$, $p_s(t)$, and $u_s(t)$ are defined similarly in the following form

$$y_s(t) = \begin{bmatrix} y(t-s) \\ \vdots \\ y(t-1) \\ y(t) \end{bmatrix} \tag{6}$$

Further, $m_s = (s+1)m$, $n_s = (s+1)n$, $l_s = (s+1)l$, and $s \le n$ is the observability index.

Defining

$$z_s(t) = \begin{bmatrix} y_s(t) \\ u_s(t) \end{bmatrix} \in \Re^{m_s + l_s}, \tag{7}$$

we can rewrite Eq. 2 as

$$[I \quad -H_s] z_s(t) = \Gamma_s x(t-s) - H_s v_s(t) + G_s p_s(t) + o_s(t) \tag{8}$$

If a sensor is faulty, its measurement will contain the normal values of the process variables and the fault. Therefore, we represent the input and output sensor faults as follows

$$z_s(t) = z_s^*(t) + \Xi_i f_i(t) \tag{9}$$

where

$$z_s^*(t) = \begin{bmatrix} y_s^*(t) \\ u_s^*(t) \end{bmatrix}$$

is the fault-free portion of the variables. The matrix $\Xi_i \in \Re^{(m_s + l_s) \times l_i}$ is orthogonal representing the fault direction and $f_i(t) \in \Re^{l_i}$ is the fault magnitude vector. To represent a single sensor fault $l_i = s+1$ and Ξ_i is an $(m_s + l_s) \times (s+1)$ matrix, which is multidimensional. This is different from the static fault detection case in Qin and Li (1999) where a single sensor fault is unidimensional. Furthermore, actuator faults can also be represented in this form, but in this article we mainly consider sensor faults.

Since s is the observability index, it is necessary and sufficient to have $(s+1)$ blocks in the matrix Γ_s and Eq. 8 in order to completely represent the redundancy of the process. This can be shown by denoting the characteristic polynomial of A as

$$|\lambda I_n - A| = \sum_{k=1}^{n} a_k \lambda^k$$

and denoting

$$\Phi = [a_0 I_m, a_1 I_m, \ldots, a_s I_m]$$

The Cayley-Hamilton theorem gives

$$\Phi \Gamma_s = \mathbf{0}$$

Therefore, premultiplying Eq. 8 by Φ gives

$$\Phi[I \quad -H_s] z_s(t) = \Phi[-H_s v_s(t) + G_s p_s(t) + o_s(t)] \tag{10}$$

which is equal to zero in the absence of noise. Equation 10 provides m equalities to represent the redundancy among the input-output variables. If more than $(s+1)$ blocks are included in Γ_s, the additional blocks will be dependent on the first $(s+1)$ blocks. If fewer than $(s+1)$ blocks are included in Γ_s, the represented redundant equations could be less than the number of outputs m, which is insufficient.

Fault detection

To use Eq. 8 for fault detection, we must eliminate the unknown state vector $x(t-s)$. We denote $\Gamma_s^{\perp} \in \Re^{m_s \times (m_s - n)}$ as the orthogonal complement of Γ_s with linearly independent columns such that

$$\left(\Gamma_s^{\perp}\right)^T \Gamma_s = \mathbf{0}$$

Pre-multiplying Eq. 8 by $(\Gamma_s^{\perp})^T$ leads to

$$B_s z_s(t) = e(t) \in \Re^{m_s - n} \tag{11}$$

where

$$B_s \equiv \left(\Gamma_s^{\perp}\right)^T [I \quad -H_s] \tag{12}$$

$$e(t) \equiv \left(\Gamma_s^{\perp}\right)^T [-H_s v_s(t) + G_s p_s(t) + o_s(t)] \tag{13}$$

Chow and Willsky (1984) used this model to eliminate unknown states. This technique of eliminating unknown variables is also used in Crowe et al. (1983) for steady-state data reconciliation.

The matrix $\Gamma_s^{\perp}$ can be derived in several ways. If the process matrices $\{A, B, C, D\}$ are known, then we can choose $(\Gamma^{\perp})^T = \Phi$ using the Cayley-Hamilton theorem. In the case that an SMI method is used to identify the model, we need only to identify B_s directly from the data, avoiding the need to estimate the $\{A, B, C, D\}$ matrices. This approach is more practical and will be discussed in detail later.

Substituting Eq. 9 into Eq. 11 gives

$$\begin{aligned} e(t) &= B_s[z_s^*(t) + \Xi_i f_i(t)] \\ &= e^*(t) + B_s \Xi_i f_i(t) \end{aligned} \tag{14}$$

where $e^*(t) = e(t)|_{f_i = \mathbf{0}} = -H_s v_s(t) + G_s p_s(t) + o_s(t)$ is the model residual under normal conditions. Since $e^*(t)$ contains the measurement noise and process noise which are Gauss-

ian, $e^*(t)$ is also Gaussian (Anderson, 1984)

$$e^*(t) \sim \mathfrak{N}(\mathbf{0}, \boldsymbol{R}_e) \tag{15}$$

Consequently,

$$e^{*T}(t)\boldsymbol{R}_e^{-1}e^*(t) \sim \chi^2(m_s - n) \tag{16}$$

where

$$\boldsymbol{R}_e \equiv E\{e^*(t)e^{*T}(t)\}$$

is the covariance matrix of $e^*(t)$ and can be estimated from the normal process data. Therefore, we can define the following fault detection index

$$d = e^T(t)\boldsymbol{R}_e^{-1}e(t) \tag{17}$$

when its confidence limit is $d_\alpha = \chi_\alpha^2(m_s - n)$, where α is the level of significance.

To reduce the effect of noise in the model residual, an exponentially weighted moving average (EWMA) filter can be applied to $e(t)$ as follows,

$$\bar{e}(t) = \gamma\bar{e}(t-1) + (1-\gamma)e(t) \tag{18}$$

where $0 \le \gamma < 1$. From Eq. 18, it directly follows that

$$\bar{e}(t) = (1-\gamma)\sum_{j=0}^{\infty}\gamma^j e(t-j)$$

which is also normally distributed. Therefore, we define a filtered detection index

$$\bar{d} = \bar{e}^T(t)\bar{\boldsymbol{R}}_e^{-1}\bar{e}(t) \sim \chi^2(m_s - n) \tag{19}$$

where $\bar{\boldsymbol{R}}_e$ is the covariance matrix of $\bar{e}(t)$ which can also be estimated from the filtered process data. If, for a new sample, $\bar{d} \le \chi_\alpha^2(m_s - n)$, the process is normal; otherwise, a fault has been detected.

Extension to other forms of dynamic models

Although the DSRAMS is proposed in terms of a subspace model, it can also be applied to many types of dynamic models, such as state space, ARX, and FIR models. If the state space matrices $\boldsymbol{A}$, $\boldsymbol{B}$, $\boldsymbol{C}$, and $\boldsymbol{D}$ are available, we can simply convert them into $\boldsymbol{\Gamma}_s$ and $\boldsymbol{H}_s$ using Eqs. 3 and 4. Then, we can calculate the subspace model $\boldsymbol{B}_s$ based on $\boldsymbol{\Gamma}_s$ and $\boldsymbol{H}_s$. If the system model is described by the following ARX model

$$y(t) + \boldsymbol{A}_1 y(t-1) + \cdots + \boldsymbol{A}_{m_y} y(t-m_y) = \boldsymbol{B}_1 u(t-1) + \cdots + \boldsymbol{B}_{m_u} u(t-m_u) + v(t)$$

we can use the following augmented matrix

$$\left[\boldsymbol{I}, \boldsymbol{A}_1, \ldots, \boldsymbol{A}_{m_y}, -\boldsymbol{B}_1, \ldots, -\boldsymbol{B}_{m_u}\right] \tag{20}$$

to replace the subspace model $\boldsymbol{B}_s$ in Eq. 11. If the system model is described by an FIR model, we can replace the subspace model in Eq. 11 by

$$\left[\boldsymbol{I}, -\boldsymbol{B}_1, \ldots, -\boldsymbol{B}_{m_u}\right] \tag{21}$$

Fault Identification with Maximized Sensitivity

After the detection of a fault, the faulty sensors must be identified subsequently. Gertler and Singer (1990) developed a *structured residual* approach that isolates faults by rotating the model residuals to generate a set of structured residuals. A structured residual is designed so that it is insensitive to one fault or a group of faults, while sensitive to others. The design logic for all possible faults forms an incidence matrix which relates the faults to the set of structured residuals. For example, for the case of four sensors, the incidence matrix which is insensitive to one fault while sensitive to others has the following form

	f_1	f_2	f_3	f_4
r_1	0	1	1	1
r_2	1	0	1	1
r_3	1	1	0	1
r_4	1	1	1	0

where 0 means insensitive and 1 means sensitive. To maximize the ability to isolate different faults, Qin and Li (1999) propose a structured residual approach with *maximized sensitivity* (SRAMS) for steady-state processes. In the SRAMS method the structured residuals are designed to be insensitive to one group of faults, while being *most* sensitive to others using available degrees of freedom. The resulting structured residuals are unique in this design. In this section, we extend the SRAMS method to the case of dynamic processes, deriving a *dynamic structured residual approach with maximized sensitivity* (DSRAMS).

Dynamic SRAMS method

For static model-based fault detection and identification, a single sensor fault affects only one element of the measurement vector. However, for the dynamic model-based fault identification, even a single sensor fault affects multiple elements of the measurement vector $z_s(t)$, resulting in a multidimensional fault. Therefore, we present the DSRAMS fault identification method for the case of multidimensional faults, which considers single sensor faults as a special case.

For multidimensional faults, the product matrix $\boldsymbol{B}_s\boldsymbol{\Xi}_i$ in Eq. 14 can have linearly dependent columns even though $\boldsymbol{\Xi}_i$ is orthogonal. In this case, we perform singular value decomposition (SVD) for this matrix

$$\boldsymbol{B}_s\boldsymbol{\Xi}_i = \boldsymbol{U}_i\boldsymbol{D}_i\boldsymbol{V}_i^T \tag{22}$$

where $U_i \in \Re^{(m_s-n)\times \tilde{l}_i}$, $V_i \in \Re^{(m_s+l_s)\times \tilde{l}_i}$, $D_i \in \Re^{\tilde{l}_i \times \tilde{l}_i}$ contains the non-zero singular values, and $\tilde{l}_i$ is the number of non-zero singular values. Equation 14 can be rewritten as

$$\begin{aligned} e(t) &= e^*(t) + U_i D_i V_i^T f_i(t) \\ &\equiv e^*(t) + U_i \tilde{f}_i(t) \end{aligned} \tag{23}$$

where

$$\tilde{f}_i(t) \equiv D_i V_i^T f_i(t) \tag{24}$$

is the fault magnitude projected on U_i.

To identify faulty sensors using DSRAMS, we need to generate a set of structured residuals in which the ith residual $r_i(t)$ is insensitive to a group of sensor faults (including the ith sensor fault) and most sensitive to others. Defining

$$\begin{aligned} r_i(t) &= w_i^T e(t) \\ &= w_i^T e^*(t) + w_i^T U_i \tilde{f}_i(t) \end{aligned} \tag{25}$$

where $w_i \in \Re^{m_s-n}$ must be orthogonal to the columns of U_i while having minimum angles to the columns of other fault matrices U_j for $j \neq i$. Mathematically, this criterion to design w_i for $i = 1, \ldots, m_f$, where m_f is the total number of faults, is equivalent to

$$\max_{w_i} \sum_{j=1}^{m_f} \| U_j^T w_i \|^2 \tag{26}$$

subject to

$$U_i^T w_i = \mathbf{0} \quad \text{and} \quad \| w_i \| = 1$$

Therefore, we choose w_i in the orthogonal complement of U_i, that is

$$w_i = \left(I - U_i U_i^T\right) \omega_i \tag{27}$$

The objective (Eq. 26) now becomes

$$\max_{\omega_i} \sum_{j=1}^{m_f} \| U_j^T \left(I - U_i U_i^T\right) \omega_i \|^2 = \max_{\omega_i} \sum_{j=1}^{m_f} \| U_{ji}^T \omega_i \|^2 \tag{28}$$

subject to

$$\| \left(I - U_i U_i^T\right) \omega_i \| = 1 \tag{29}$$

where

$$U_{ji} \equiv \left(I - U_i U_i^T\right) U_j \tag{30}$$

is the projection of U_j on the orthogonal complement of U_i. Applying a Lagrange multiplier, ω_i is found to be the solution to the following equation

$$\sum_{j=1}^{m_f} U_{ji} U_{ji}^T \omega_i = \lambda \left(I - U_i U_i^T\right) \omega_i \tag{31}$$

Rearranging Eq. 30, we obtain

$$U_{ji} = \left(I - U_i U_i^T\right) U_j = \left(I - U_i U_i^T\right)^2 U_j = \left(I - U_i U_i^T\right) U_{ji}$$

Therefore, Eq. 31 becomes

$$\sum_{j=1}^{m_f} U_{ji} U_{ji}^T \left(I - U_i U_i^T\right) \omega_i = \lambda \left(I - U_i U_i^T\right) \omega_i \tag{32}$$

Using Eq. 27 again we have

$$\sum_{j=1}^{m_f} U_{ji} U_{ji}^T w_i = \lambda w_i \tag{33}$$

Therefore, w_i is simply the eigenvector of $\sum_{j=1}^{m_f} U_{ji} U_{ji}^T$ associated with the largest eigenvalue. Note that only this largest eigenvalue satisfies the sufficient condition for the objective in Eq. 28 to achieve the maximum.

It should be noted that one can design a structured residual to be insensitive to several sensor faults while most sensitive to others, as long as there are enough degrees of freedom available. One must satisfy the isolability condition in this design (Gertler and Singer, 1990). The detailed algorithm is similar to the one described previously, except that several fault direction matrices should be included in Eq. 22.

Fault identification indices

After the structured residuals are generated, decision about which sensor fails has to be made. Due to modeling errors, measurement noise and other uncertainties, the residuals $r_i(t)$ are not equal to zero. From Eq. 25, we can infer that if there is no fault

$$r_i(t) = w_i^T e^*(t) \sim \mathfrak{N}\left(0, w_i^T R_e w_i\right) \quad i = 1, 2, \ldots, m_f. \tag{34}$$

If the jth fault occurs, the residuals

$$r_i(t) \sim \begin{cases} \mathfrak{N}\left(0, w_i^T R_e w_i\right) & \text{if } i = j, \\ \mathfrak{N}\left(\mu_{ij}, w_i^T R_e w_i\right) & \text{if } i \neq j. \end{cases}$$

where

$$\mu_{ij} = w_i^T U_j \tilde{f}_j(t) \tag{35}$$

Consequently, if there is no fault

$$\frac{r_i^2(t)}{w_i^T R_e w_i} \sim \chi^2(1) \tag{36}$$

Therefore, we could use $r_i^2(t)$ as a fault identification index.

In order to reduce the effect of random noise and modeling errors, these residuals often need to be filtered before being used for fault identification. Further, several types of indices are required to be sensitive to different types of faults. For example, using a low-pass filter will identify bias type of faults easily, but it will not be sensitive to faults with high frequency changes. On the other hand, a fault identification index without filtering will give false identification due to noise. Qin and Li (1999) provide four types of indices to deal with this issue: (i) an EWMA filtered structured residual (FSR); (ii) a generalized likelihood ratio (GLR) based on the structured residuals; (iii) a cumulative sum (Qsum) of the structured residuals; and (iv) a cumulative variance (Vsum) index. The EWMA based FSR provides smoothing to the residuals so that high frequency noise will not cause false alarms. The GLR and Qsum are essentially equivalent which use a rectangular moving window to filter the noise. The Vsum index is specifically designed to identify precision-degradation faults which have large variance changes.

EWMA Filtered Structured Residuals. When an EWMA filter is applied to $r_i(t)$, the filtered structured residual is

$$\bar{r}_i(t) = \gamma \bar{r}_i(t-1) + (1-\gamma) r_i(t) \sim \mathfrak{N}\left(0, \boldsymbol{w}_i^T \bar{\boldsymbol{R}}_e \boldsymbol{w}_i\right) \quad (37)$$

when there is no fault. When the jth fault occurs, we can use the following FSR index to identify the faulty sensor

$$I_{FSR}^i(t) \equiv \frac{\bar{r}_i^2(t)}{\boldsymbol{w}_i^T \bar{\boldsymbol{R}}_e \boldsymbol{w}_i \, \chi_\alpha^2(1)} \begin{cases} \le 1 \text{ if } i = j, \\ > 1 \text{ if } i \ne j \end{cases}.$$

This will allow us to identify the faulty sensor.

Generalized Likelihood Ratios. If a sensor fault incurs significant changes in the mean such as bias or drift, the generalized likelihood ratio test is usually appropriate to use (Benveniste et al., 1987; Basseville et al., 1993). If sensor j is faulty, the GLR for the ith structured residual is (Qin and Li, 1999)

$$S_t(\hat{\mu}_{ij}) = \frac{t_\omega \hat{\mu}_{ij}^2}{\boldsymbol{w}_i^T \boldsymbol{R}_e \boldsymbol{w}_i} \sim \chi^2(1), \quad \text{for } i = j \quad (38)$$

because

$$\hat{\mu}_{ij} = \frac{1}{t_w} \sum_{k=t-t_w+1}^{t} r_i(k) \quad (39)$$

$$\sim \mathfrak{N}\left(0, \frac{\boldsymbol{w}_i^T \boldsymbol{R}_e \boldsymbol{w}_i}{t_w}\right), \quad \text{for} \quad i = j$$

where $[t-t_w+1, t]$ is the time window that include the faulty period and t_w the window width. Therefore, if sensor j is faulty

$$\begin{cases} S_t(\hat{\mu}_{ij}) \le \chi_\alpha^2(1) & \text{for} \quad i = j, \\ S_t(\hat{\mu}_{ij}) > \chi_\alpha^2(1) & \text{for} \quad i \ne j. \end{cases}$$

We then define a GLR index as follows

$$I_{\text{GLR}}^i(t) = \frac{S_t(\hat{\mu}_{ij})}{\chi_\alpha^2(1)} \quad (40)$$

Under normal conditions, $I_{\text{GLR}}^i(t)$ $(i = 1, 2, \ldots, m_f)$ are less than one. If sensor j is faulty, $I_{\text{GLR}}^i(t)$ will be less than one for $i = j$, but all other $I_{\text{GLR}}^i(t)$ $(i \ne j)$ will be larger than one.

Cumulative Variance Index. If a sensor incurs a precision degradation fault (that is, mainly variance changes), both FSR and GLR will have difficulty identifying it. In this case, we can use a cumulative variance index

$$V_{\text{sum}}^i(t) = \sum_{k=t-t_w+1}^{t} \left[r_i(k) - \hat{\mu}_{ij}\right]^2, \quad i = 1, 2, \ldots, m_f \quad (41)$$

Under normal conditions, the following ratio follows a Chi-square distribution with $(t_w - 1)$ degree of freedom (Hald, 1952)

$$\frac{V_{\text{sum}}^i(t)}{\boldsymbol{w}_i^T \boldsymbol{R}_e \boldsymbol{w}_i} \sim \chi^2(t_w - 1)$$

Therefore, we define a normalized index for Vsum,

$$I_{V\text{sum}}^i(t) = \frac{V_{\text{sum}}^i(t)}{\boldsymbol{w}_i^T \boldsymbol{R}_e \boldsymbol{w}_i \, \chi_\alpha^2(t_w - 1)} \quad (42)$$

A value above one for this index indicates an abnormal situation. If sensor j is faulty

$$\begin{cases} I_{V\text{sum}}^i(t) \le 1 \text{ for } i = j, \\ I_{V\text{sum}}^i(t) > 1 \text{ for } i \ne j. \end{cases}$$

Fault estimation

With the presence of a sensor fault, as shown by Eq. 14, $\boldsymbol{e}(t)$ increases in magnitude. Since the fault direction has been identified, we choose a time function $\hat{f}_i(t)$ in the direction of $\boldsymbol{B}_s \boldsymbol{\Xi}_i$ to minimize the effect of the fault on $\boldsymbol{e}(t)$, that is, to minimize

$$J = \| \boldsymbol{e}^*(t) \|^2 = \| \boldsymbol{e}(t) - \boldsymbol{B}_s \boldsymbol{\Xi}_i f_i(t) \|^2 \quad (43)$$

A least-squares estimate for the fault magnitude based on Eq. 22 is

$$\hat{f}_i(t) = (\boldsymbol{B}_s \boldsymbol{\Xi}_i)^+ \boldsymbol{e}(t) \quad (44)$$

$$= \boldsymbol{V}_i \boldsymbol{D}_i^{-1} \boldsymbol{U}_i^T \boldsymbol{e}(t) \quad (45)$$

where $()^+$ stands for the Moore-Penrose pseudo inverse (Albert, 1972). Note that $\hat{f}_i(t)$ contains the estimates of the fault values consecutively from $t-s$ through t. Since we are usu-

ally interested in estimating the current fault value, we only need to compute the associated rows in $\hat{f}_i(t)$.

Isolating sensor faults from process changes

Although the ultimate objective of this work is to detect and identify sensor faults, process changes, whether normal or abnormal, can interfere with the sensor validation results and cause false alarms. Therefore, it is important to distinguish sensor faults from process changes.

Typically, process changes can be classified into three categories:

(i) unmeasured, normal process disturbances;

(ii) slow process degradation which may or may not lead to a process fault; and

(iii) abnormal process changes which prohibit the process from functioning normally.

These process changes can be further divided into two types: additive and multiplicative changes. For example, leakage in a pipeline system is a typical additive fault, while a process parameter variation is a typical multiplicative fault. Unmeasured process disturbances can affect the process either as an additive change (such as ventilation) or as a multiplicative change (such as inlet concentration). In principle, both additive and multiplicative changes affect the residuals differently from sensor faults. Therefore, they can be distinguished from sensor faults. To deal with the effect of additive changes $d(t) \in \Re^{m_d}$, we can write $e(t)$ and the structured residuals as follows assuming that no sensor faults occur

$$z_s(t) = z_s^*(t) - \Xi_d d(t)$$

$$e(t) = B_s z_s^*(t) + B_s \Xi_d d(t)$$

$$r_i(t) = w_i^T B_s z_s^*(t) + w_i^T B_s \Xi_d d(t) \quad i = 1, 2, \ldots, m_f \quad (46)$$

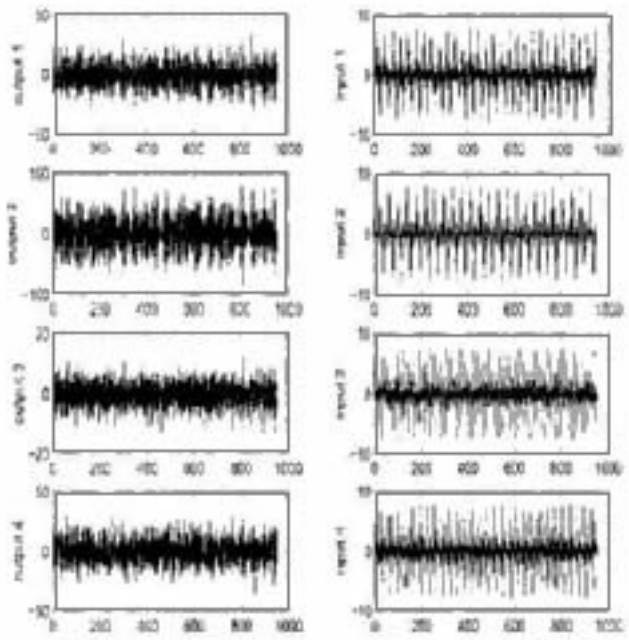

Figure 1. Process data for a simulated 4×4 process.

where Ξ_d is the direction in which the process fault affects the measurement. As long as Ξ_d does not overlap with any one of the sensor fault directions Ξ_i, *all* structured residuals are affected by the fault. Therefore, based on this analysis, we can distinguish sensor faults from process disturbances or faults.

Multiplicative process faults typically lead to a change in the process model. For example, we can have the process matrix

$$B_{s,p} = B_s + \Delta B_s$$

The structured residuals are still generated based on the model matrix B_s, that is

$$r_i(t) = w_i^T B_s z_s(t) = w_i^T B_{s,p} z_s(t) - w_i^T \Delta B_s z_s(t)$$

$$= w_i^T e_s^*(t) - w_i^T \Delta B_s z_s(t)$$

The first term on the righthand side of the above equation is random noise that defines the confidence limit, while the second term is the effect of multiplicative process changes.

Since the process parameter change ΔB_s is typically unknown before hand and does not coincide with a sensor fault direction, multiplicative process changes will affect all residuals $r_i(t)$ for $i = 1, \ldots, m_f$. Therefore, multiplicative process faults can also be distinguished from sensor faults. In summary, if the fault detection index detects a faulty situation, and all structured residuals are affected, it is likely a process change instead of a sensor fault.

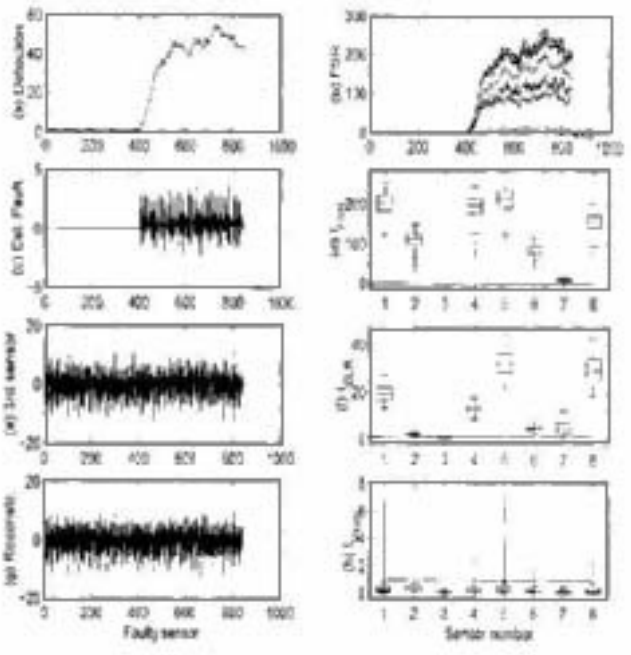

Figure 2. Fault detection, identification, and reconstruction results for a bias in output sensor 3 of a simulated 4×4 process.

Consistent Estimation of the EIV Subspace Model

In order to carry out the fault detection and identification task, we must have a dynamic model of the normal process as given in Eq. 1. One way of building such a state space model is to use subspace identification methods. Recently, many types of subspace identification algorithms are available (such as, Van Overschee and De Moor, 1994). Because most of them assume that the system input is noise-free (Verhaegen, 1994; Van Overschee and De Moor, 1994), these algorithms give biased estimates for the EIV model in Eq. 1 (Chou and Verhaegen, 1997).

To identify a consistent model from noisy input-output observations, Moonen et al. (1989) propose an EIV subspace-based identification method using quotient singular value decomposition (QSVD). This scheme gives estimates of the system matrices $\{A, B, C, D\}$ under the assumption that the input and output are corrupted with white noise. The EIV SMI algorithm proposed by Chou and Verhaegen (1997) allows cross-correlation in the noise terms

$$E\left\{\begin{bmatrix} p(t) \\ v(t) \\ o(t) \end{bmatrix}\begin{bmatrix} p^T(j) & v^T(j) & o^T(j) \end{bmatrix}\right\} = \begin{bmatrix} \Sigma_p & \Sigma_{pv} & \Sigma_{po} \\ \Sigma_{pv}^T & \Sigma_v & \Sigma_{vo} \\ \Sigma_{po}^T & \Sigma_{vo}^T & \Sigma_o \end{bmatrix}\delta_{t,j} \quad (47)$$

where $\delta_{t,j}$ is the Kronecker Delta function.

Most of the SMI methods involve two steps in the identification: (1) estimate the subspace of the extended observability matrix Γ_s and the Toeplitz matrix H_s; and (2) estimate $\{A, B, C, D\}$ from the extended matrices. For the purpose of fault detection and identification, however, we only need to identify the matrix B_s in Eq. 11. Since from Eq. 12

$$B_s = \begin{bmatrix} \left(\Gamma_s^{\perp}\right)^T & -\left(\Gamma_s^{\perp}\right)^T H_s \end{bmatrix} \quad (48)$$

we propose an EIV method to identify B_s by estimating $-(\Gamma_s^{\perp})^T H_s$ and $(\Gamma_s^{\perp})^T$ directly from noisy input and output data.

Given corrupted input and output measurements $\{u(t)\}$ and $\{y(t)\}$ for $t = 1, 2, \ldots, N+2s$, we can formulate the following block Hankel matrices

$$U_t = \begin{bmatrix} u_s(t+s) u_s(t+s+1) \cdots u_s(t+s+N-1) \end{bmatrix} = \begin{bmatrix} u(t) & u(t+1) & \cdots & u(t+N-1) \\ u(t+1) & u(t+2) & \cdots & u(t+N) \\ \vdots & \vdots & \ddots & \vdots \\ u(t+s) & u(t+s+1) & \cdots & u(t+s+N-1) \end{bmatrix} \in \Re^{l_s \times N} \quad (49)$$

and

$$Y_t = \begin{bmatrix} y_s(t+s) y_s(t+s+1) \cdots y_s(t+s+N-1) \end{bmatrix} = \begin{bmatrix} y(t) & y(t+1) & \cdots & y(t+N-1) \\ y(t+1) & y(t+2) & \cdots & y(t+N) \\ \vdots & \vdots & \ddots & \vdots \\ y(t+s) & y(t+s+1) & \cdots & y(t+s+N-1) \end{bmatrix} \in \Re^{m_s \times N} \quad (50)$$

for $t = 1$ and $t = s+1$. Similarly, we can define a matrix

$$Z_t = \begin{bmatrix} Y_t^T & U_t^T \end{bmatrix}^T$$

From Eq. 2 it is straightforward to have

$$Y_t = \Gamma_s X_t + H_s U_t - H_s V_t + G_s P_t + O_t \quad (51)$$

where $X_t = [x(t)\ x(t+1) \cdots x(t+N-1)]$, the noise matrices U_t, V_t and O_t have the same block Hankel form as Y_t, and the noise terms are finitely correlated according to Eq. 47.

Setting $t = s+1$ in Eq. 51 and post-multiplying it by $1/N(Z_1^T)$ give rise to

$$\frac{1}{N} Y_{s+1} Z_1^T = \frac{1}{N}\Gamma_s X_{s+1} Z_1^T + \frac{1}{N} H_s U_{s+1} Z_1^T - \frac{1}{N} H_s V_{s+1} Z_1^T + \frac{1}{N} G_s P_{s+1} Z_1^T + \frac{1}{N} O_{s+1} Z_1^T \quad (52)$$

We now examine the last three terms of the prior equation. These three terms will vanish to zero as $N \to \infty$, because the future noises V_{s+1}, P_{s+1}, and O_{s+1} are independent of past

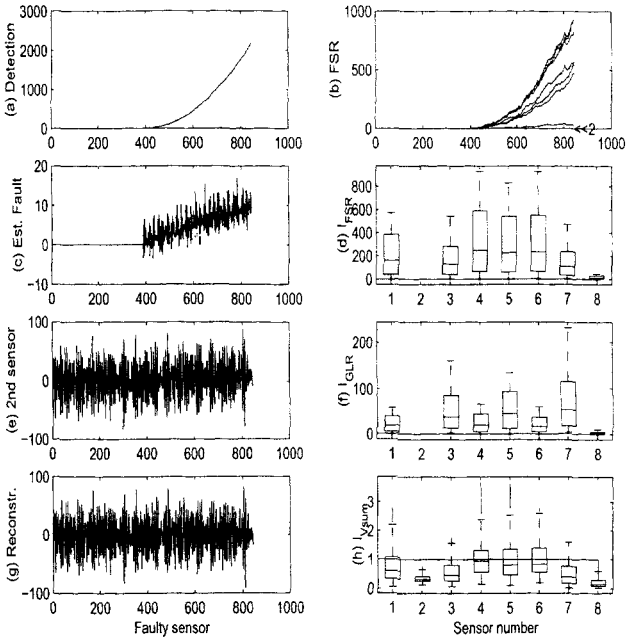

Figure 3. Fault detection, identification, and reconstruction results for a drift in output sensor 2 of a simulated 4×4 process.

data Z_1^T (Chou and Verhaegen, 1997). Therefore, we have as N tends to infinity,

$$K_{YZ} = \frac{1}{N}\Gamma_s X_{s+1} Z_1^T + H_s K_{UZ} \tag{53}$$

where

$$K_{YZ} \equiv \frac{1}{N} Y_{s+1} Z_1^T \in \Re^{m_s \times (m_s + l_s)}$$

and

$$K_{UZ} \equiv \frac{1}{N} U_{s+1} Z_1^T \in \Re^{l_s \times (m_s + l_s)}$$

Since our objective is to estimate $(\Gamma_s^{\perp})^T$ and $(\Gamma_s^{\perp})^T H_s$ from process data, we eliminate the last term in Eq. 53 by post-multiplying it with

$$\Pi_{UZ}^{\perp} = I - K_{UZ}^{+} K_{UZ},$$

which is a projection to the orthogonal complement of K_{UZ}, we obtain

$$K_{YZ}\Pi_{UZ}^{\perp} = \frac{1}{N}\Gamma_s X_{s+1} Z_1^T \Pi_{UZ}^{\perp} \tag{54}$$

From Eq. 54 it is clear that $K_{YZ}\Pi_{UZ}^{\perp}$ has the same subspace as Γ_s. Therefore, by performing SVD on $K_{YZ}\Pi_{UZ}^{\perp}$

$$K_{YZ}\Pi_{UZ}^{\perp} = \begin{bmatrix} U_\Gamma & U_\Gamma^{\perp} \end{bmatrix} \begin{bmatrix} D_\Gamma & 0 \\ 0 & 0 \end{bmatrix} \begin{bmatrix} V_\Gamma & V_\Gamma^{\perp} \end{bmatrix}^T$$

$$= U_\Gamma D_\Gamma V_\Gamma^T \tag{55}$$

where D_Γ is a diagonal matrix containing non-zero singular values of $K_{YZ}\Pi_{UZ}^{\perp}$, $\Gamma_s^{\perp}$ can be chosen as $\Gamma_s^{\perp} = U_\Gamma^{\perp}$.

After $\Gamma_s^{\perp}$ is identified, pre-multiplying it on Eq. 53 gives

$$\left(\Gamma_s^{\perp}\right)^T K_{YZ} = \left(\Gamma_s^{\perp}\right)^T H_s K_{UZ} \tag{56}$$

Therefore,

$$\left(\Gamma_s^{\perp}\right)^T H_s = \left(\Gamma_s^{\perp}\right)^T K_{YZ} K_{UZ}^{+} \tag{57}$$

We note that the pseudo-inverse is necessary when K_{UZ} does not have full row rank. This can happen if the inputs are collinear or not persistently excited to the order $s+1$. The lack of persistent excitation is typical when the data are collected from normal operations, that is, without designed experiments. If the data were collected under a designed experiment which makes K_{UZ} full row rank, $K_{UZ}^{+} = K_{UZ}^T (K_{UZ} K_{UZ}^T)^{-1}$.

Summarizing the above derivation, we formulate the following subspace identification algorithm for estimating B_s. Note that this algorithm gives a *consistent* estimate for B_s under the EIV assumption (Chou and Verhaegen, 1997).

(1) Select an initial estimate of the process order n, and set $s = n$.

(2) Formulate data matrices, Z_1, Y_{s+1}, U_{s+1}, and calculate K_{UZ}, K_{YZ} and $\Pi_{UZ}^{\perp}$.

(3) Perform SVD on $K_{YZ}\Pi_{UZ}^{\perp}$ according to Eq. 55 and set $\Gamma_s^{\perp} = U_\Gamma^{\perp}$.

(4) Set $n = \dim\{D_\Gamma\}$ and $s = n$. Repeat steps 2 and 3 once.

(5) Calculate $(\Gamma_s^{\perp})^T H_s$ based on Eq. 57. The model matrix is given in Eq. 48.

Case Studies

Simulated 4 × 4 process

To test the effectiveness of the proposed method, we simulate a 4×4 dynamic process with two state variables. The process model matrices are

$$A = \begin{bmatrix} 0.67 & 0.67 \\ -0.67 & 0.67 \end{bmatrix}$$

$$B = \begin{bmatrix} -0.4326 & 0.1253 & -1.1465 & 1.1892 \\ -1.6656 & 0.2877 & 1.1909 & -0.0376 \end{bmatrix}$$

$$C = \begin{bmatrix} 0.3273 & -0.5883 \\ 0.1746 & 2.1832 \\ -0.1867 & -0.1364 \\ 0.7258 & 0.1139 \end{bmatrix}$$

$$D = \begin{bmatrix} 1.0668 & 0.2944 & -0.6918 & -1.4410 \\ 0.0593 & -1.3362 & 0.8580 & 0.5711 \\ -0.0956 & 0.7143 & 1.2540 & -0.3999 \\ -0.8323 & 1.6236 & -1.5937 & 0.6900 \end{bmatrix}$$

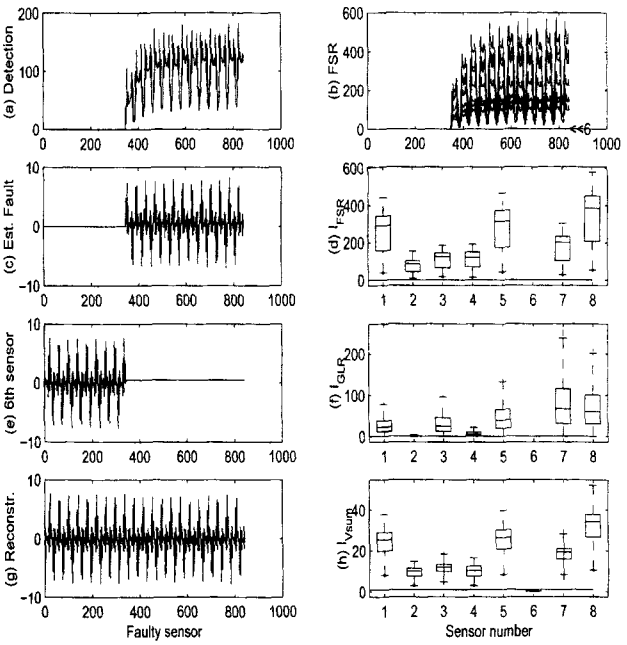

Figure 4. Fault detection, identification, and reconstruction results for a complete failure in input sensor 2 of a simulated 4×4 process.

The process inputs are perturbed with a multitude of sinusoidal signals with various frequencies. Both input and output variables are subject to measurement noise and the process is subject to process noise. This situation makes it necessary to use errors-in-variables identification methods, as proposed in this article. The noise terms are all Gaussian white noise.

Normal process data, which are shown in Figure 1, are generated and scaled to zero mean and unit variance to apply equal weighting to all variables. Using the subspace identification algorithm depicted earlier in this article, Γ_s is estimated as

$$\hat{\Gamma}_s = \begin{bmatrix} -0.2430 & 0.3333 \\ 0.0114 & -0.4744 \\ 0.2773 & 0.2692 \\ -0.4417 & -0.1261 \\ -0.3937 & 0.0493 \\ 0.3363 & -0.2949 \\ 0.0155 & 0.3387 \\ -0.2164 & -0.3921 \\ -0.3115 & -0.2036 \\ 0.4404 & 0.0193 \\ -0.2265 & 0.2160 \\ 0.1067 & -0.3593 \end{bmatrix}$$

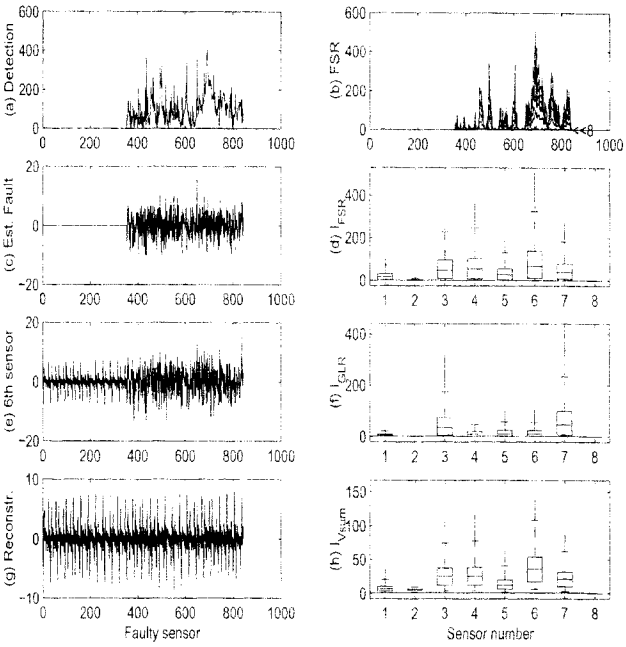

Figure 5. Fault detection, identification, and reconstruction results for a precision degradation in input sensor 4 of a simulated 4×4 process.

The vectors w_i for $i = 1, \cdots, 8$ that generate the structured residuals are given in each row of the following matrix

$$W = \begin{bmatrix} 0.25 & -0.74 & 0.09 & -0.12 & 0.24 & -0.43 & 0.08 & -0.29 & -0.15 & 0.10 \\ 0.27 & -0.61 & 0.20 & -0.28 & 0.07 & -0.06 & 0.57 & -0.12 & -0.04 & 0.29 \\ 0.27 & 0.74 & -0.11 & -0.11 & 0.19 & 0.11 & 0.49 & 0.20 & 0.17 & 0.03 \\ 0.38 & 0.10 & -0.03 & 0.07 & 0.52 & -0.47 & 0.58 & -0.11 & 0.00 & 0.02 \\ 0.43 & -0.29 & 0.08 & -0.11 & 0.39 & -0.37 & 0.58 & -0.23 & -0.04 & 0.17 \\ 0.13 & 0.65 & -0.21 & 0.40 & 0.36 & -0.34 & 0.20 & 0.02 & -0.06 & -0.25 \\ 0.13 & 0.76 & 0.02 & -0.12 & 0.06 & 0.33 & 0.51 & 0.12 & 0.05 & 0.07 \\ 0.18 & -0.50 & -0.06 & 0.22 & 0.39 & -0.67 & -0.10 & -0.20 & -0.10 & -0.11 \end{bmatrix}$$

The confidence limits for fault detection and identification indices are also calculated before performing online fault detection and identification.

Faulty data are simulated by introducing one of four types of faults: bias, drift, complete failure and precision degradation. In each case, fault occurrence t_f is varied. For each type of faults, after the detection index $\bar{d}(t)$ triggers an alarm, three identification indices are used to identify the faulty sensor. An EWMA filter with a coefficient $\gamma = 0.98$ is applied to generate the FSRs. The GLR and Vsum indices are calculated based on the unfiltered structured residuals with a moving window of 31 samples.

A bias $f_{y,3}(t) = 0.4$ is introduced to the output sensor 3 at $t_f = 400$. The fault detection and identification results are shown in Figure 2: (a) fault detection index; (b) FSRs plotted over time; (c) estimated fault magnitude; (d), (f), and (h) box-whisker plots for FSRs, GLRs, and Vsum indices against their confidence limits; (e) original faulty sensor; and (g) reconstructed values for the faulty sensor. The filtered fault detection index effectively detects the fault as $t = 407$. Among all fault identification indices, the FSR and GLR indices are effective in identifying that sensor 3 is the faulty sensor, while the Vsum is not effective as expected.

A drift type fault is introduced to output sensor 2 as follows

$$f_{y,2}(t) = 0.02(t - t_f), \quad t \geq t_f \tag{58}$$

where the fault time $t_f = 355$. The fault detection and identification results are depicted in Figure 3. Similar to the bias fault case, the FSR and GLR indices are effective in identifying that sensor 2 is the fault sensor. The Vsum index is not effective at all as expected.

A complete failure is introduced to input sensor 2 by assuming that $u_2(t) = 0.5$ is constant after the time instant $t_f = 344$. The fault detection and identification results are depicted in Figure 4. In this case fault detection index detects the fault at $t = 345$. Further, all three identification indices are effective in uniquely identifying that input sensor 2 (sensor number 6) is the faulty sensor in this case. The fault reconstruction effectively restores the normal values of the input sensor 2.

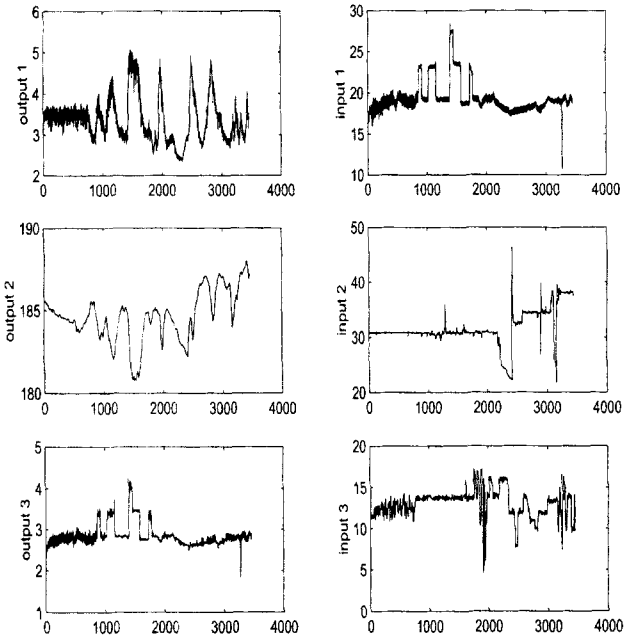

Figure 6. Process data for an industrial 3×3 process.

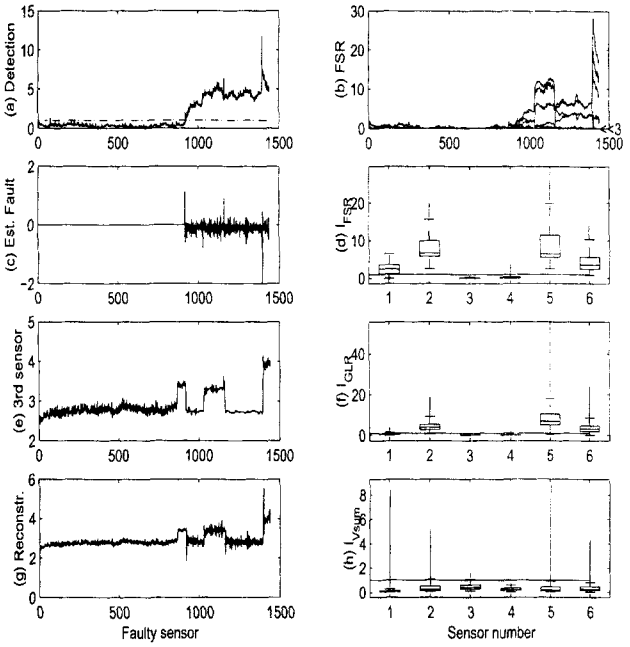

Figure 7. Fault detection, identification, and reconstruction results for a bias in output sensor 3 of an industrial reactor.

A variance degradation fault is simulated by adding zero mean Gaussian random sequence with variance $\sigma^2 = 4.0$ to input sensor 4 at $t_f = 355$. The fault detection and identification results are depicted in Figure 5. The fault detection index immediately detects the fault. Among the three identification indices the only effective one is Vsum, which uniquely indicates that the input sensor 4 (sensor number 8) is faulty. In summary, FSR and GLR indices are effective for all types of faults other than variance degradation; Vsum is the most effective for variance degradation faults only.

Industrial reactor process

The proposed fault detection and identification scheme is applied to an industrial reactor process, which has three inputs and three output variables. Raw data are collected, as shown in Figure 6, and scaled to zero mean and unit variance to apply equal weighting to all variances. Using the subspace identification algorithm proposed in the previous section, we find that this reactor process can be represented by a third-order state space model. Before conducting fault detection and identification, we calculated $\Gamma_s^{\perp}$, w_i for $i = 1, \ldots, 6$, and the confidence limits for fault detection and identification indices.

Faulty data are simulated by introducing one of four types of faults: bias, drift, complete failure, and precision degradation to one sensor at a time. In each case, the fault occurrence instant t_f is varied.

For each type of faults, after the detection index $\bar{d}(t)$ triggers an alarm, three identification indices are used to identify the faulty sensor. An EWMA filter with a coefficient $\gamma = 0.98$ is applied to generate the FSRs. The GLR and Vsum indices are calculated based on the unfiltered structured residuals with a moving window of 31 samples.

A bias $f_{y,3}(t) = -0.1$ is introduced to the output sensor 3 at $t_f = 900$. The fault detection and identification results are shown in Figure 7: (a) fault detection index; (b) FSRs plotted over time; (c) estimated fault magnitude; (d), (f), and (h) box-whisker plots for FSRs, GLRs, Vsum indices against their confidence limits; (e) original faulty sensor; and (g) reconstructed values for the faulty sensor. While the detection index effectively detects the fault at $t = 918$, the FSR index is most effective in identifying the bias fault among the three identification indices. It is seen that sensors 3 and 4 are both

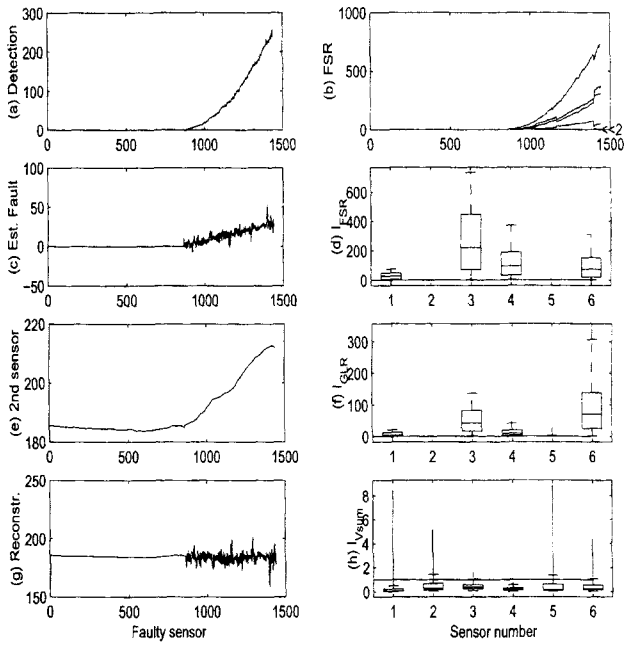

Figure 8. Fault detection, identification, and reconstruction results for a drift in output sensor 2 of an industrial reactor.

below the threshold and are identified as the faulty sensors. Further examination of the process indicates that these two sensors are almost exactly collinear as shown in Figure 6. Although the identification is not unique, it effectively narrows down the scope for further diagnosis.

A drift type fault is introduced to output sensor 2 as follows,

$$f_{y,2}(t) = 0.05(t - t_f), \quad t \geq t_f \tag{59}$$

where the fault time $t_f = 850$. The fault detection and identification results are depicted in Figure 8. The fault detection index detects the fault at $t = 863$. Similar to the bias fault case, the FSR index is most effective in identifying that sensors 2 and 5 are possibly faulty. The Vsum index is not effective at all as expected. The fault reconstruction results are shown in sub-figure (g), although the reconstruction is noisy.

A complete failure is introduced to input sensor 1 by assuming that $u_1(t) = 18$ is constant after the instant $t_f = 900$. The fault detection and identification results are depicted in Figure 9. In this case the fault detection index detects the fault immediately. The FSR index is most effective in identifying that sensors 3 and 4 are possible faulty sensors. The ambiguity is due to the fact that sensors 3 and 4 are exactly collinear. Vsum index is not effective. The fault reconstruction effectively restores the normal values of sensor 4.

A variance degradation fault is simulated by adding zero mean Gaussian random sequence with variance $\sigma^2 = 2.0$ to input sensor 2 at $t_f = 900$. The fault detection and identification results are depicted in Figure 10. It is seen that the only effective identification index is Vsum, which uniquely indicates that the input sensor 2 (sensor number 5) is faulty. In summary, FSR is most effective for all types of fault other than variance degradation; Vsum is most effective for variance degradation faults only. The combined use of these indices can help identify the faulty sensors and fault types. Since there are collinearity among some variables, unique identification of faulty sensors may not be possible as demonstrated in this real process.

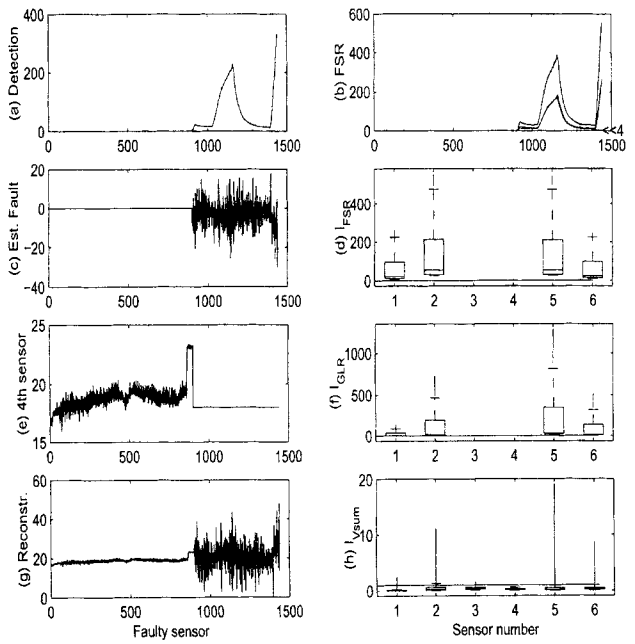

Figure 9. Fault detection, identification, and reconstruction results for a complete failure in input sensor 1 of an industrial reactor.

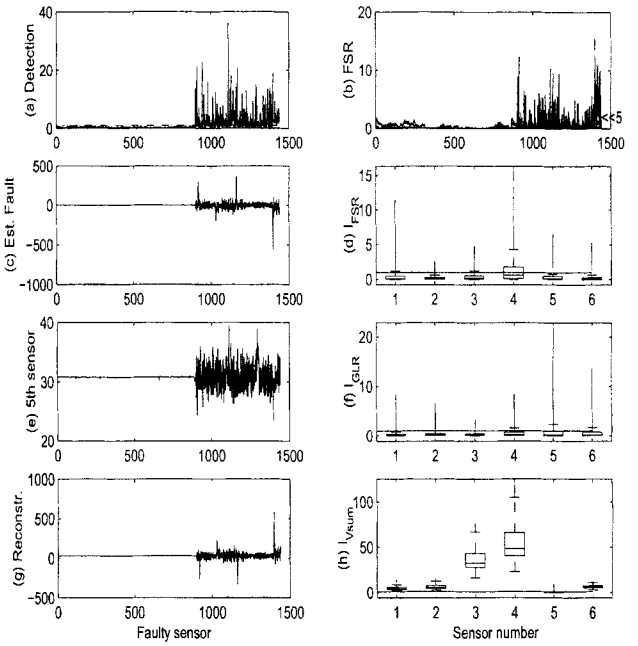

Figure 10. Fault detection, identification, and reconstruction results for a precision degradation in input sensor 3 of an industrial reactor.

Conclusions

A novel dynamic sensor fault identification scheme is proposed based on structured residuals and subspace models. The structured residual approach is enhanced with maximized sensitivity to some faults, while being decoupled from others. The proposed error-in-variables subspace identification algorithm provides a consistent subspace model suitable for fault detection and identification. Using the subspace model, both fault detection and fault identification indices are decoupled from the process states, which avoids the need for state estimation. An EWMA filter is used to pre-process the model residual for fault detection and structured residuals for fault identification in order to reduce the effects of measurement noise. Statistical methods to determine the alarm thresholds for both fault detection and identification are developed. The proposed method is successfully applied to a simulated dynamic process and an industrial reactor process with satisfactory results. Four types of sensor faults, bias, drift, complete failure, and precision degradation are tested with three fault identification indices: FSR, GLR, and Vsum. Comparisons of these indices on one industrial process and one simulated process indicate that Vsum is most effective to variance changes, while FSR is most effective to other types of faults. Future work is seen in the derivation of fault identifiability conditions in dynamic systems.

Acknowledgments

The authors acknowledge the financial support from Aspen Tech and National Science Foundation CAREER Grant (CTS-9985074) for this work and the technical discussions with Dr. John Guiver from Aspen Tech during the progress of this work.

Literature Cited

Albert, A., *Regression and the Moore-Penrose Pseudoinverse*, Academic Press, New York (1972).

Albuquerque, J. S., and L. T. Biegler, "Data Reconciliation and Gross-Error Detection for Dynamic Systems," *AIChE J.*, **42**, 2841 (1996).

Anderson, T. W., *An Introduction to Multivariate Statistical Analysis*, 2nd ed., Wiley, New York (1984).

Basseville, M., and I. V. Nikiforov, *Detection of Abrupt Changes—Theory and Applications*, Prentice-Hall, Englewood Cliffs, NJ (1993).

Benveniste, A., M. Basseville, and G. Moustakides, "The Asymptotic Local Approach to Change Detection and Model Validation," *IEEE Trans. Auto. Cont.*, **32**, 583 (July 1987).

Chou, C., and M. Verhaegen, "Subspace Algorithms for the Identification of Multivariable Dynamic Errors-in-Variables Models," *Automatica*, **33**, 1857 (1997).

Chow, E., and A. Willsky, "Analytical Redundancy and the Design of Robust Failure Detection Systems," *IEEE Trans. Auto. Cont. AC-29*, 603 (1984).

Crowe, C., "Data Reconciliation—Progress and Challenges," *J. Proc. Cont.*, **6**, 89 (1996).

Crowe, C., A. Hrymak, and Y. A. G. Campos, "Reconciliation of Process Flow Rates by Matrix Projection. i. The Linear Case," *AIChE J.*, **29**, 881 (1983).

Deckert, J., M. Desai, J. Deyst, and A. Willsky, "F-8 DFBW Sensor Failure Identification Using Analytical Redundancy," *IEEE Trans. Auto. Cont.*, **AC-22**, 796 (1977).

Dunia, R., J. Qin, T. F. Edgar, and T. J. McAvoy, "Identification of Faulty Sensors Using Principal Component Analysis," *AIChE J.*, **42**, 2797 (1996).

Fantoni, P., and A. Mazzola, "Applications of Autoassociative Neural Networks for Signal Validation in Accident Management," *Proceedings of the IAEA Specialist Meeting on Advanced Information Methods and Artificial Intelligence in Nuclear Power Plant Control Rooms* (1994).

Frank, P., and J. Wunnenberg, "Robust Fault Diagnosis Using Unknown Input Observer Schemes," *Fault Diagnosis in Dynamic Systems*, R. Patton, P. Frank, and R. Clark, eds., Prentice-Hall, Englewood Cliffs, NJ (1989).

Frank, P. M., and X. Ding, "Survey of Robust Residual Generation and Evaluation Methods in Observer-Based Fault Detection Systems," *J. Proc. Cont.*, **7**, 403 (1997).

Gertler, J., "Analytical Redundancy Method in Fault Detection and Isolation, Survey and Synthesis," *Proceedings of the IFAC SAFEPROCESS Symp.* (Sept. 10–13, 1991).

Gertler, J., W. Li, Y. Huang, and T. McAvoy, "Isolation-Enhanced Principal Component Analysis," *AIChE J.*, **45**, 323 (1999).

Gertler, J., and D. Singer, "A New Structural Framework for Parity Equation Based Failure Detection and Isolation," *Automatica*, **26**, 381 (1990).

Gertler, J. J., and M. M. Kunwer, "Optimal Residual Decoupling for Robust Fault Diagnosis," *Int. J. Control*, **61**, 395 (1995).

Hald, A., *Statistical Theory with Engineering Applications*, John Wiley & Sons, Inc. (1952).

Jackson, J. E., *A User's Guide to Principal Components*, Wiley-Interscience, New York (1991).

Karjala, T. W., and D. M. Himmelblau, "Dynamic Rectification of Data Via Recurrent Neural Nets and the Extended Kalman Filter," *AIChE J.*, **42**, 2225 (1996).

Kresta, J. V., J. F. MacGregor, and T. E. Marlin, "Multivariate Statistical Monitoring of Processes," *Can. J. Chem. Eng.*, **69**, 35 (1991).

Liebman, M., T. Edgar, and L. Lasdon, "Efficient Data Reconciliation and Estimation for Dynamic Processes Using Nonlinear Programming Techniques," *Comput. Chem. Eng.*, **16**, 963 (1992).

Mah, R. S. H., G. M. Stanley, and D. Downing, "Reconciliation and Rectification of Process Flow and Inventory Data," *Ind. Eng. Chem. Proc. Des. Dev.*, **15**, 175 (1976).

Miller, P., R. Swanson, and C. Heckler, "Contribution Plots: The Missing Link in Multivariate Quality Control," *Fall Conf. of the ASQC and ASA*, Milwaukee, WI (1993).

Moonen, M., B. DeMoor, L. Vandenberghe, and J. Vandewalle, "On and Off-Line Identification of Linear State-Space Models," *Int. J. of Control*, **49**, 219 (1989).

Qin, S. J., and W. Li, "Detection, Identification and Reconstruction of Faulty Sensors with Maximized Sensitivity," *AIChE J.*, **45**, 1963 (1999).

Rollins, D. K., and J. F. Davis, "Unbiased Estimation of Gross Errors in Process Measurements," *AIChE J.*, **38**, 563 (1992).

Romagnoli, J. A., and G. Stephanopoulos, "Rectification of Process Measurement Data in the Presence of Gross Errors," *Chem. Eng. Sci.*, **36**, 1849 (1981).

Stanley, G. M., and R. S. H. Mah, "Estimation of Flows and Temperatures in Process Networks," *AIChE J.*, **23**, 642 (1977).

Stanley, G. M., and R. S. H. Mah, "Observability and Redundancy in Process Data Estimation," *Chem. Eng. Sci.*, **36**, 259 (1981).

Tong, H., and C. M. Crowe, "Detection of Gross Errors in Data Reconciliation by Principal Component Analysis," *AIChE J.*, **41**, 1712 (1995).

Van Overschee, P., and B. D. Moor, "Subspace Algorithms for the Identification of Combined Deterministic-Stochastic Systems," *Automatica*, **30**, 75 (1994).

Verhaegen, M., "Identification of the Deterministic Part of MIMO State Space Models Given in Innovations Form from Input-Output Data," *Automatica*, **30**, 61 (1994).

Manuscript received Feb. 16, 2000, and revision received Jan. 22, 2001.